Eur. Phys. J. C 36, 315–321 (2004)
Digital Object Identifier (DOI) 10.1140/epjc/s2004-01965-3

THE EUROPEAN PHYSICAL JOURNAL C

# A measurement of $\Xi^-$ polarization in inclusive production by $\Sigma^-$ of 340 GeV/c in C and Cu targets

The WA89 Collaboration

M.I. Adamovich[8,†], Yu.A. Alexandrov[8,a], S.P. Baranov[8,a], D. Barberis[3], M. Beck[5], C. Bérat[4], W. Beusch[2], M. Boss[6], S. Brons[5,b], W. Brückner[5], M. Buénerd[4], Ch. Busch[6], Ch. Büscher[5], F. Charignon[4], J. Chauvin[4], E.A. Chudakov[6,c], U. Dersch[5], F. Dropmann[5], J. Engelfried[6,d], F. Faller[6,e], A. Fournier[4], S.G. Gerassimov[6,8,f], M. Godbersen[5], P. Grafström[2], Th. Haller[5], M. Heidrich[5], E. Hubbard[5], R.B. Hurst[3], K. Königsmann[5,g], I. Konorov[5,8,f], N. Keller[6], K. Martens[6,h], Ph. Martin[4], S. Masciocchi[5,i], R. Michaels[5,c], U. Müller[7], H. Neeb[5], D. Newbold[1], C. Newsom[j], S. Paul[5,f], J. Pochodzalla[5,k] B. Povh[5], R. Ransome[l], Z. Ren[5], M. Rey-Campagnolle[4,m], G. Rosner[7,n], L. Rossi[3], H. Rudolph[7], L. Schmitt[7,f], H.-W. Siebert[6], A. Simon[6,g], V.J. Smith[1,o], O. Thilmann[6,p], A. Trombini[5], E. Vesin[4], B. Volkemer[7], K. Vorwalter[5], Th. Walcher[7], G. Wälder[6], R. Werding[5], E. Wittmann[5], M.V. Zavertyaev[8,q,a]

[1] Univ. of Bristol, Bristol BS8 1TL, UK
[2] CERN, 1211 Genève 23, Switzerland
[3] Dipt. di Fisica and INFN, 16146 Genova, Italy
[4] Inst. de Sciences Nucléaires, Univ. Grenoble, 38026 Grenoble, France
[5] Max-Planck-Inst. für Kernphysik, 69029 Heidelberg, Germany
[6] Physikalisches Institut, Univ. Heidelberg, 69120 Heidelberg, Germany[r]
[7] Inst. für Kernphysik, Univ. Mainz, 55099 Mainz, Germany[r]
[8] P.N. Lebedev Physics Inst., 117924, Moscow, Russia

Received: 17 Febraury 2004 / Revised version: 9 June 2004 /
Published online: 23 July 2004 – 

**Abstract.** We have measured the polarization of $\Xi^-$ hyperons produced inclusively by a $\Sigma^-$ beam of 340 GeV/c momentum in nuclear targets. From a sample of 880000 identified $\Xi^-$ decays, polarizations were determined in the range $0 < x_F < 0.9$ and $p_t \leq 1.6$ GeV/c. The polarization w.r.t. the production normal is negative for $x_F \geq 0.3$. At fixed values of $x_F$, its magnitude increases with $p_t$ to maximum values which reach about 20% at large $x_F$.

## 1 Introduction

It is well known that hyperons produced in high-energy hadronic reactions are polarized transverse to the production plane. While details of this process still are not understood, the existing data show differences based on whether the strange quark content of the produced hyperon was created from the sea or whether a strange quark was trans-

[a] supported by Deutsche Forschungsgemeinschaft, contract number DFG 436 RUS 113/465/0-2(R), and Russian Foundation for Basic Research under contract number RFFI 00-02-04018
[b] Now at TRIUMF, Vancouver, B.C., Canada V6T 2A3
[c] Now at Thomas Jefferson Lab, Newport News, VA 23606, USA
[d] Now at Instituto de Fisica, Universidad Autonoma de San Luis Potosi, S.L.P. 78240 Mexico
[e] Now at Fraunhofer Inst. für Solar Energiesysteme,79100 Freiburg, Germany.
[f] Now at Physik Dept. E18, TU München, 85747 Garching, Germany
[g] Now at Fakultät für Physik, Univ. Freiburg, Germany
[h] Now at Physics Dept., Univ. of Utah, Salt Lake City, Utah, USA
[i] Now at Max-Planck-Institut für Physik, München, Germany
[j] University of Iowa, Iowa City, IA 52242, USA
[k] Now at Inst. für Kernphysik, Univ. Mainz, Germany
[l] Rutgers University, Piscataway, NJ 08854, USA
[m] permanent address: CERN, 1211 Genève 23, Switzerland
[n] Now at Dept. of Physics and Astronomy, Univ. of Glasgow, Glasgow G128QQ, UK
[o] supported by the UK PPARC
[p] Now at Dept. of Radiation Physics, Lund Univ., 22185 Lund, Sweden
[q] Now at Max-Planck-Inst. für Kernphysik, Heidelberg, Germany
[r] supported by the Bundesministerium für Bildung, Wissenschaft, Forschung und Technologie, Germany, under contract numbers 05 5HD15I, 06 HD524I and 06 MZ5265
[†] deceased

ferred from the beam projectile. It is therefore desirable to have polarization data not only for produced hyperons of different strangeness, but also for beam projectiles of different strangeness. The bulk of the existing polarization data comes from inclusive $\Lambda$ production, mostly in proton beam experiments, but there exist also data from neutron, $\pi^-$ and $K^-$ beams. Data on polarization in $\Sigma$, $\Xi$ and $\Omega^-$ production again come mainly from proton beam experiments, but $\Xi^-$ and $\Omega^-$ polarization has also been measured in a neutral beam containing neutrons, $\Lambda$ and $\Xi^0$. For reviews of the experimental and theoretical situation see for instance [1–5].

Further insights into the role of the valence quark content of the beam particle may arise from experiments which use high-intensity beams of $\Sigma^-$. We present here the results of a polarization study based on a sample of 880000 identified $\Xi^- \to \Lambda\pi^-$ decays produced by a $\Sigma^-$ beam of 340 GeV/c mean momentum in copper and carbon targets. These data were recorded in 1993 and 1994 in the CERN hyperon beam experiment WA89. Results on $\Lambda$ polarizations based on the same data have already been published [6]. In a previous study of $\Lambda$, $\overline{\Lambda}$, $\Sigma^+$ and $\Xi^-$ polarizations based on a smaller sample recorded in 1991 in the same experiment [7] we found negative $\Xi^-$ polarizations with magnitudes up to 30% at large $p_t$.

Previous measurements of the polarization of $\Xi^-$ and $\Xi^0$ produced inclusively in proton beams of 400 and 800 GeV/c momentum [8–10] showed negative $\Xi^-$ polarization, increasing in magnitude with $p_t$ up to $p_t = 1\,GeV/c$ with a plateau of $|P| \approx 0.15$ at higher $p_t$ values, with no significant difference between $\Xi^-$ and $\Xi^0$ and similar to the behaviour of $\Lambda$ polarization. In contrast, $\Xi^-$ produced in an unpolarized neutral beam mainly by $\Xi^0$ showed polarizations compatible with zero at a level of 1% [11].

There are no quantitative predictions of $\Xi^-$ polarization in inclusive production by $\Sigma^-$. The fragmentation/recombination model of DeGrand and Miettinen [12] predicts that the sign of the polarization should be negative as in $\Lambda$ production by protons.

## 2 Hyperon beam and experimental apparatus

The hyperon beam and the apparatus are described in our previous publication on $\Lambda$ polarization [6], therefore only a short description is given here.

The hyperon beam was derived from an external proton beam of the CERN-SPS at 450 GeV/c momentum, which hit a Be target. A magnetic channel selected negatively charged secondaries emerging from this target at production angles of less than 1 mrad. This ensured that the hyperons in the secondary beam had a negligible polarization. The mean beam momentum was 345 GeV/$c$ and 330 GeV/$c$ in the beam periods 1993 and 1994, respectively, and the momentum spread was $\sigma(p)/p \approx 9\%$.

The secondary beam was directed onto the experiment target 16m downstream. There the beam consisted of $\pi^-$, $K^-$, $\Sigma^-$ and $\Xi^-$ in the ratio $2.3 : 0.025 : 1 : 0.013$. Typically, about $1.8 \cdot 10^5$ $\Sigma^-$ and $4.2 \cdot 10^5$ $\pi^-$ were delivered to the target during one SPS-spill of 1.5 sec duration. A transition radiation detector (TRD) allowed $\pi^-$ to be suppressed at the trigger level. A detailed description of the hyperon beam can be found in [13].

The experiment target consisted of one copper and three carbon blocks arranged in a row along the beam, with thicknesses corresponding to 0.026 and three times 0.0083 interaction lengths, respectively, with the copper block positioned upstream of the carbon blocks. The tracks of the incoming beam particle and of the charged particles produced in the target blocks were measured in microstrip detectors. The momenta of the incoming beam particles, however, could not be measured individually.

The experiment target was positioned 14m upstream of the centre of the Omega spectrometer magnet [14] so that a field-free decay region of 10m length was provided for hyperon and $K_S$ decays. The Omega magnet provided a field integral of 7.5 Tm. Tracks of charged particles were measured inside the magnet and in the field-free regions immediately upstream and downstream by MWPCs and drift chambers; the momentum resolution achieved was $\sigma(p)/p^2 \approx 10^{-4}$ $(\mathrm{GeV}/c)^{-1}$.

A ring-imaging Cherenkov detector, an electromagnetic calorimeter and a hadron calorimeter were located downstream of the spectrometer, but these components were not used in this analysis.

The main trigger selected about 25% of all interactions. Correlations between hits in different detectors were used to increase the fraction of events with high-momentum particles, thus reducing background from low-momentum pions in the beam. The results presented in this article are based on 200 million events recorded in 1993 and 1994.

## 3 Selection of $\Xi^-$ decays

The requirements on the identification of the $\Xi^-$ production vertex were the same as for $\Lambda$ production: Each accepted event had to have a single incoming beam track and an interaction vertex containing at least two outgoing charged tracks, all tracks being reconstructed in the microstrip counters around the experiment target. The beam track had to intercept the production vertex at a distance of less than 500 $\mu$m, to suppress interactions of neutrons and $\Lambda$ from $\Sigma^-$ and $\Xi^-$ decays upstream of the target. To suppress interactions of particles scattered from the collimator walls, the position/direction correlation for beam particles coming directly from the proton target had to be fulfilled.

The identification of $\Lambda \to p\pi^-$ decays from the measured p and $\pi^-$ tracks was straightforward and is described in [6]. The effective ($p\pi^-$) mass had to be within $\pm$ 10 MeV/$c^2$ of the $\Lambda$ mass.

$\Xi^-$ candidates then were selected by using any additional negative track with measured momentum to reconstruct the $\Xi^-$ direction and decay vertex. The reconstructed $\Lambda$ line-of-flight and the $\pi^-$ track had to have a distance of $< 5\,mm$ at the reconstructed $\Xi^-$ decay vertex. Furthermore it was required that the reconstructed $\Xi^-$

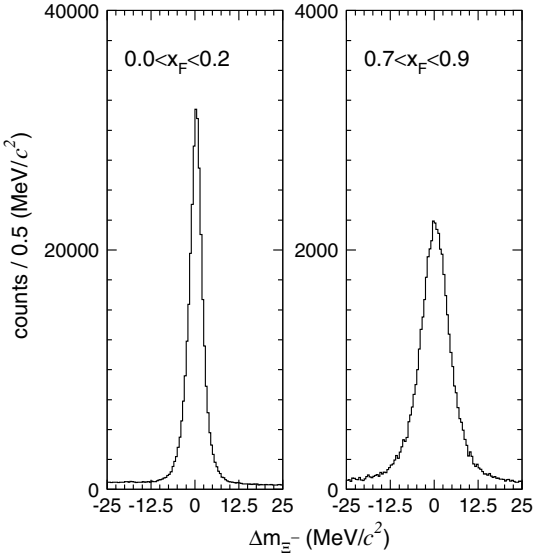


**Fig. 1.** $\Delta m_{\Xi}$, the difference between the effective $\Lambda\pi^-$ effective mass and the $\Xi^-$ mass. Event numbers are per 0.5 MeV/$c^2$. Left: $0 < x_F < 0.2$, right: $0.7 < x_F < 0.9$

track agreed in angle and position with a track observed in the microstrip detectors downstream of the target. The agreement was quantified in a quality factor $Q_{\Xi}$ based on the position and direction differences between the reconstructed track and the observed track. Requiring this factor to be less than 2.5 rejected about 5% of all genuine $\Xi^-$.

Figure 1 shows the distributions of the effective $(\Lambda\pi^-)$ mass for $\Xi^-$ candidates with $0 < x_F < 0.2$ (left) and $0.7 < x_F < 0.9$ (right). The r.m.s. of the $\Xi^-$ mass peaks can be parametrized as $\sigma_m^2 = a^2 + (b \cdot p_\Lambda)^2$, with the contribution from multiple scattering being a = 2.2 MeV/$c^2$ and the contribution from coordinate measurement errors being $b \cdot p_\Lambda = 1.5$ MeV/$c^2$ at $p_\Lambda = 100$ GeV/c. $\Xi^-$ candidates had to have a $\Lambda\pi^-$ effective mass within $\pm 2\,\sigma_m$ of the $\Xi^-$ mass. At low $p_t$, the background/signal ratio within this signal window increases with $x_F$ from 0.10 to 0.15 and at high $p_t$ from 0.01 to 0.06. After subtraction of a linear background taken from "side windows" inside ± 24 MeV/$c^2$, a sample of 880,000 $\Xi^- \to \Lambda\pi^-$ decays remained in the range $0 < x_F < 0.9$. $\Xi^-$ candidates with $x_F > 0.9$ were rejected because of the presence of $\Xi^-$ in the beam.

## 4 Polarization analysis

The polarizations were measured w.r.t. the direction of the production normal $\hat{n} \propto \hat{p}_{\rm beam} \times \hat{p}_{\Xi}$, using the relation $f(cos\vartheta^*_\Lambda) \propto 1 + A \cdot cos\vartheta^*_\Lambda$, where $A = P_\Xi \cdot \alpha_\Xi$ is the product of the $\Xi^-$ polarization and decay parameter and $\vartheta^*_\Lambda$ is the angle between the production normal and the direction of the daughter $\Lambda$ in the $\Xi^-$-CMS. $\alpha_\Xi$ = -0.458 is the $\Xi^-$ decay parameter [15]. The beam particle direction $\hat{p}_{\rm beam}$ was measured individually.

We used a coordinate system with the symmetry axis of the experiment as the x-direction. The beam particle directions coincided with the x-axis to within 2 mrad. The y-axis pointed horizontally to the left, looking downstream, and the z-axis pointed vertically upwards. In this geometry, the production normal was confined to the y-z plane and had an azimuth $\varphi_n = \varphi_\Xi + 90^o$.

**Table 1.** Polarization results I. The statistics of the $\Xi^-$ signal is after background subtraction. $p_t$ is in units of GeV/c

| sample | $\Xi^-$ sample | | mean | mean | polarization | |
|---|---|---|---|---|---|---|
| no. | signal | bgrd. | $x_F$ | $p_t$ | [%] | $\chi^2_{\rm sectors}$ |
| 1 | 15386 | 1634 | 0.09 | 0.13 | −2.4±3.8 | 2.5 |
| 2 | 38198 | 1728 | 0.09 | 0.31 | −0.2±2.8 | 2.2 |
| 3 | 43212 | 1300 | 0.09 | 0.50 | −0.8±2.7 | 1.6 |
| 4 | 35962 | 737 | 0.09 | 0.70 | −5.2±2.8 | 1.5 |
| 5 | 24292 | 393 | 0.09 | 0.89 | −11.1±3.1 | 2.3 |
| 6 | 14087 | 200 | 0.10 | 1.09 | −3.6±3.8 | 0.4 |
| 7 | 13818 | 141 | 0.10 | 1.43 | −6.8±3.8 | 0.5 |
| 8 | 16126 | 1483 | 0.20 | 0.13 | −5.0±3.7 | 0.3 |
| 9 | 40039 | 1682 | 0.20 | 0.31 | −2.2±2.8 | 1.7 |
| 10 | 45385 | 1497 | 0.20 | 0.50 | −0.4±2.7 | 0.1 |
| 11 | 34737 | 891 | 0.20 | 0.69 | −2.6±2.9 | 0.2 |
| 12 | 22872 | 487 | 0.20 | 0.89 | −2.9±3.3 | 0.2 |
| 13 | 13277 | 239 | 0.20 | 1.09 | 4.6±3.9 | 0.6 |
| 14 | 15593 | 195 | 0.20 | 1.44 | −8.1±3.7 | 6.9 |
| 15 | 13783 | 1403 | 0.30 | 0.13 | −1.9±4.0 | 0.4 |
| 16 | 34450 | 1468 | 0.30 | 0.31 | −2.9±2.9 | 0.9 |
| 17 | 40498 | 1388 | 0.30 | 0.50 | −2.3±2.8 | 1.7 |
| 18 | 32521 | 957 | 0.30 | 0.69 | −6.5±2.9 | 1.6 |
| 19 | 20260 | 495 | 0.30 | 0.89 | −11.5±3.3 | 3.6 |
| 20 | 10981 | 259 | 0.30 | 1.09 | −7.6±4.2 | 3.0 |
| 21 | 11088 | 222 | 0.30 | 1.44 | −13.6±4.2 | 0.1 |
| 22 | 11232 | 1299 | 0.40 | 0.13 | 1.2±4.4 | 0.5 |
| 23 | 26588 | 1236 | 0.40 | 0.31 | −1.2±3.1 | 4.7 |
| 24 | 31252 | 1227 | 0.40 | 0.50 | −4.2±3.0 | 0.9 |
| 25 | 25500 | 844 | 0.40 | 0.69 | −6.4±3.1 | 7.7 |
| 26 | 16199 | 521 | 0.40 | 0.89 | −16.3±3.6 | 0.1 |
| 27 | 8628 | 264 | 0.40 | 1.09 | −14.7±4.6 | 1.0 |
| 28 | 7695 | 200 | 0.40 | 1.42 | −15.2±4.9 | 0.3 |

The polarizations were determined in 7x7 bins of $x_F$ and $p_t$, as listed in Tables 1 and 2. "Feynman-x" $x_F$ is defined as $x_F = 2p_\ell^{CM}/\sqrt{s}$, where $\sqrt{s}$ is the invariant mass of the (beam - target nucleon) system and $p_\ell^{CM}$ is the $\Xi^-$ momentum in beam particle direction in the (beam - target nucleon) CMS. $p_t$ is the $\Xi^-$ momentum transverse to the beam particle direction.

### 4.1 Bias cancelling

Biases resulting from unrecognized apparatus asymmetries are the main cause for worry in any polarization measurement. For instance, the Omega magnet bent positively/negatively charged particles to the left/right, thereby introducing a strong acceptance bias in favour of $\pi^-$ emission to the left. If not properly taken into account, this acceptance bias would translate into a positive polariza-

**Table 2.** Polarization results II

| sample | $\Xi^-$ sample | | mean | mean | polarization | |
|---|---|---|---|---|---|---|
| no. | signal | bgrd. | $x_F$ | $p_t$ | [%] | $\chi^2_{\text{sectors}}$ |
| 29 | 8243 | 1052 | 0.50 | 0.13 | 0.3±5.0 | 2.4 |
| 30 | 19521 | 964 | 0.50 | 0.31 | 0.6±3.4 | 0.1 |
| 31 | 22986 | 1037 | 0.50 | 0.50 | −0.2±3.3 | 0.9 |
| 32 | 19053 | 788 | 0.50 | 0.69 | −9.3±3.5 | 5.1 |
| 33 | 12021 | 471 | 0.50 | 0.89 | −14.6±4.1 | 2.6 |
| 34 | 6409 | 206 | 0.50 | 1.09 | −6.8±5.2 | 7.4 |
| 35 | 5412 | 215 | 0.50 | 1.41 | −17.8±5.7 | 4.4 |
| 36 | 5827 | 753 | 0.60 | 0.13 | 3.6±5.9 | 5.5 |
| 37 | 13236 | 777 | 0.60 | 0.31 | 3.8±3.9 | 3.4 |
| 38 | 15151 | 842 | 0.60 | 0.50 | −1.3±3.8 | 4.2 |
| 39 | 12708 | 677 | 0.60 | 0.69 | −5.7±4.0 | 1.8 |
| 40 | 8018 | 361 | 0.60 | 0.89 | −9.8±4.7 | 4.6 |
| 41 | 4022 | 207 | 0.60 | 1.09 | −27.2±6.4 | 3.1 |
| 42 | 3393 | 179 | 0.60 | 1.41 | −17.0±7.1 | 0.1 |
| 43 | 6954 | 1048 | 0.75 | 0.13 | 7.2±5.4 | 0.3 |
| 44 | 14871 | 1089 | 0.74 | 0.30 | 8.6±3.8 | 0.3 |
| 45 | 15590 | 1067 | 0.74 | 0.50 | −4.2±3.8 | 0.6 |
| 46 | 12166 | 745 | 0.74 | 0.69 | 1.5±4.1 | 4.3 |
| 47 | 7155 | 441 | 0.74 | 0.89 | −5.6±5.1 | 1.3 |
| 48 | 3602 | 250 | 0.73 | 1.09 | −21.0±6.8 | 0.7 |
| 49 | 2669 | 169 | 0.73 | 1.40 | −17.1±7.9 | 0.8 |

tion bias for $\Xi^-$ emitted upwards and a corresponding negative polarization bias for $\Xi^-$ emitted downwards.

In order to cancel apparatus biases, we adopted the following procedure: to determine the polarization in a given interval of $x_F$ and $p_t$ we subdivided that $x_F/p_t$ sample into subsamples corresponding to 12 sectors of 30° in $\varphi_\Xi$. In each sector of $\varphi_\Xi$, , the polarization was determined by calculating the asymmetry $a(\cos\vartheta) = (n(\cos\vartheta) - n(-\cos\vartheta)) \,/\, (n(\cos\vartheta) + n(-\cos\vartheta))$ in 10 bins of $0 < \cos\vartheta < +1$ and then determining A from a fit to $a(\cos\vartheta) = A \cdot \cos\vartheta$. To be bias-free, this method does not require the acceptance and reconstruction efficiency $\epsilon$ to be constant, but only $\epsilon(cos\vartheta_p^*) = \epsilon(-cos\vartheta_p^*)$. The polarizations determined in each sector then were averaged to obtain bias cancellation. This method is explained in detail in [6]. As a check for the reliability of the bias cancelling, we averaged the polarizations in three subsamples of four $\varphi_\Xi$ sectors each, sample A comprising $\Xi^-$ azimuths inside $\pm 30^0$ to the vertical, sample B comprising $\Xi^-$ azimuths inside $\pm 15^0$ to the diagonals and sample C comprising $\Xi^-$ azimuths inside $\pm 30^0$ to the horizontal. If, for instance, the large left/right acceptance bias resulting from the horizontal bending of the tracks was not fully cancelled, we would expect the polarizations measured in sample A to differ systematically from the polarizations in samples B and C. Figure 2 shows the distributions of $(\text{pol}_i - \text{pol}_{\text{all}})/\sigma_i$ , where $i = A, B, C$. $\text{pol}_i$ is the polarization measured for subsample $i$ in a given $x_F/p_t$ bin, $\sigma_i$ is its statistical error and $\text{pol}_{\text{all}}$ is the polarization averaged over subsamples A, B and C. Thus each plot contains 49 entries for the 49 different $x_F/p_t$

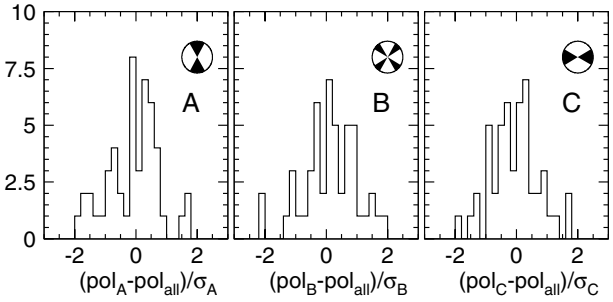


**Fig. 2.** Deviations of the polarizations measured in sector subsamples A, B and C, respectively, from the polarization averaged over all sectors. The deviations are normalized to their statistical errors. The azimuthal ranges of samples A,B and C are indicated in the corresponding figures

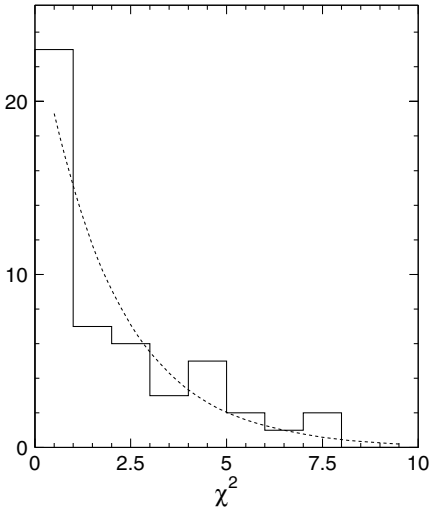


**Fig. 3.** Distribution of $\chi^2_{\text{sectors}}$. There are no overflows. The dashed curve is the $\chi^2$ distribution for 2 d.o.f.

bins. The mean values of the distributions are -0.09±0.12, +0.13±0.12 and -0.06±0.11 for A, B and C, respectively, and the observed r.m.s. values of the distributions, 0.84, 0.87 and 0.77 are in agreement with what we would expect from purely statistical fluctuations, viz. $\sigma = \sqrt{2/3} = 0.82$. To further investigate the small differences between the polarizations in A, B and C, we studied the distribution of

$$\chi^2_{\text{sectors}} = \sum_i (\text{pol}_i - \text{pol}_{\text{all}})^2/\sigma_i^2$$

which is shown in Fig. 3. $\chi^2_{\text{sectors}}$ is also listed in Tables 1 and 2. This distribution again is in good agreement with what we would expect from purely statistical fluctuations, its mean value is 2.1±0.3.

### 4.2 Search for systematic errors

As mentioned above, a cut was made on $Q_\Xi$, the quality factor describing the agreement in angle and position between a track reconstructed in the microstrip detectors downstream of the target and the $\Xi^-$ track reconstructed

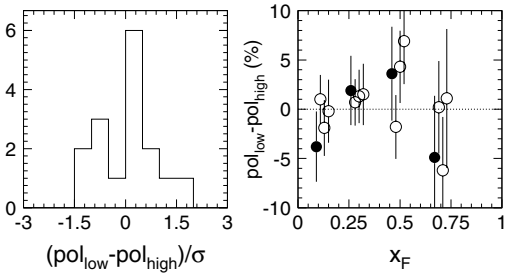


**Fig. 4.** High $Q_\Xi$/low $Q_\Xi$ comparison: The left-hand plot shows the distribution $\Delta\,\mathrm{pol}/\sigma$ for the 16 $x_F/p_t$ samples. There are no overflows. The right-hand plot shows $\Delta\,\mathrm{pol}$ in % vs $x_F$. For each value of $x_F$, four points are given corresponding to $p_t$ = 0.19 (solid) and 0.45, 0.73, 1.15 (open) from left to right, respectively

from the $\Xi^-$ decay cascade. In a search for possible biases arising from this cut, each $x_F/p_t$ sample was split by a cut on $Q_\Xi$ into two subsamples with equal statistics. The number of $x_F/p_t$ samples was reduced to 4x4 to increase the sensitivity to possible effects of this cut. Figure 4 shows on the left the distribution of $\Delta\,\mathrm{pol} = \mathrm{pol}_{\mathrm{low}} - \mathrm{pol}_{\mathrm{high}}$, normalized to the corresponding statistical errors. The r.m.s. of this distribution is 0.82 and its mean value is 0.06±0.21, in good agreement with the assumption of purely statistical fluctuations. The plot on the right shows $\Delta\,\mathrm{pol}$ as a function of $x_F$. This plot might indicate a bias of 0.01 to 0.02 depending on $x_F$. We therefore added quadratically a systematic uncertainty of ±0.02 to the statistical errors of the polarization measurements.

We have also split the $x_F/p_t$ samples into subsamples of equal size with the beam direction to the right/left or up/down resp., and for long/short $\Xi^-$ decay lengths. Comparison of these subsamples revealed no systematic differences at a level comparable to the systematic error already added to the statistical errors.

### 4.3 Beam contaminations

In the following, we investigate possible effects of beam contaminations on our results.

12% of the beam particles accepted in the trigger are fast $\pi^-$, which have the same momentum and angular distributions as the $\Sigma^-$ and were not rejected by the TRD. The cross sections for inclusive $\Xi^-$ production by $\pi^-$ and by $\Sigma^-$ have been measured simultaneously in our experiment [16]. Their ratio $r_{\pi\Sigma} = \sigma(\pi^- \to \Xi^-)/\sigma(\Sigma^- \to \Xi^-)$ decreases rapidly with $x_F$ as shown in Table 3. Even in our lowest $x_F$ bin, $0 < x_F < 0.2$, we expect that about 6% only of our $\Xi^-$ sample have been produced by $\pi^-$. Since $\Xi^-$ produced by $\pi^-$ can be expected to be essentially unpolarized as observed in $\Lambda$ production by $\pi^-$ [17] we would only have to multiply our measured polarizations by a factor $1/(1 - 0.12 \cdot r_{\pi\Sigma})$, which is negligible compared to the measurement errors.

The beam also contains an admixture of 2.2% of $K^-$. There exist no measurements of $\Xi^-$ production by $K^-$. From our experiment and from a $K^-/\pi^-$ beam experiment [18] we know that about half as many $\Lambda$ are produced by $K^-$ as by $\Sigma^-$ (see [6] for details). Assuming a similar ratio for $\Xi^-$ production by $K^-$ and $\Sigma^-$, we expect that about 1% of our $\Xi^-$ sample has been produced by $K^-$, which results in a negligible effect on our measured polarizations.

**Table 3.** Ratios of cross sections for inclusive $\Xi^-$ production in different beams: $r_{\pi\Sigma}$: pion beam / $\Sigma^-$ beam, $r_{\Xi\Sigma}$: $\Xi^-$ beam / $\Sigma^-$ beam. $f_{\Xi\Xi}$ is the fraction of $\Xi^-$ in our sample produced by $\Xi^-$

| $x_F$ | $r_{\pi\Sigma}$ | $r_{\Xi\Sigma}$ | $f_{\Xi\Xi}$ |
|---|---|---|---|
| 0.05 | 0.60 | | |
| 0.15 | 0.27 | 1.6 | 0.02 |
| 0.25 | 0.15 | 3.0 | 0.04 |
| 0.35 | 0.11 | 4.8 | 0.06 |
| 0.45 | 0.08 | 9 | 0.11 |
| 0.55 | 0.05 | 13 | 0.15 |
| 0.65 | | 19 | 0.20 |
| 0.75 | | 40 | 0.34 |
| 0.85 | | 100 | 0.57 |

The effect of the fraction of 1.3% of $\Xi^-$ contained in the beam is very different. We remind the reader that we have no possibility to tag the $\Xi^-$ in the beam individually. $\Xi^-$ production by $\Xi^-$ shows a very strong leading particle effect [19]. A comparison of $\Xi^-$ production by $\Xi^-$ and by $\Sigma^-$ is shown in Fig. 8 of [16] and the values in Table 3 are taken from this figure. At low $x_F$, the ratio $r_{\Xi\Sigma} = \sigma(\Xi^- \to \Xi^-)/\sigma(\Sigma^- \to \Xi^-)$ is about 1, but already at $x_F$=0.5 production by $\Xi^-$ is enhanced by about a factor $r_{\Xi\Sigma}$=10 and at $x_F$=0.75, the mean value of our highest $x_F$-bin, $r_{\Xi\Sigma}$=40. These ratios have an overall systematic uncertainty of 20%. Correspondingly, the fraction of $\Xi^-$ produced by $\Xi^-$ in the total $\Xi^-$ sample , $f_{\Xi\Xi}$, rises to $\approx 1/3$ at $x_F = 0.75$ (last column of Table 3).

## 5 Results

The polarization results for all $x_F/p_t$ bins are listed in Tables 1 and 2. In Fig. 5 we show the polarizations as a function of $x_F$ in fixed intervals of $p_t$ with the mean value of $p_t$ indicated in each plot. At $p_t < 0.4\,\mathrm{GeV/c}$, the polarization has a tendency to increase with $x_F$ to positive values around 5%. Above $p_t > 0.6$, the polarization changes sign and at $p_t > 0.9$ there is a clear increase of the magnitude with $x_F$ to about -20%.

In Fig. 6 we show the polarizations as a function of $p_t$ in fixed intervals of $x_F$. Except for the positive values at high $x_F$ and small $p_t$ noted above, the polarizations are negative. Above $x_F \approx 0.3$, we see the magnitude of the polarization rising with $p_t$ with no clear sign of a plateau at high $p_t$.

The results of this analysis are in good agreement with our earlier result based on 80,000 $\Xi^-$ from our 1991 data [7].

We also looked for a possible dependence of the polarization on the target nuclei. Again we have reduced the

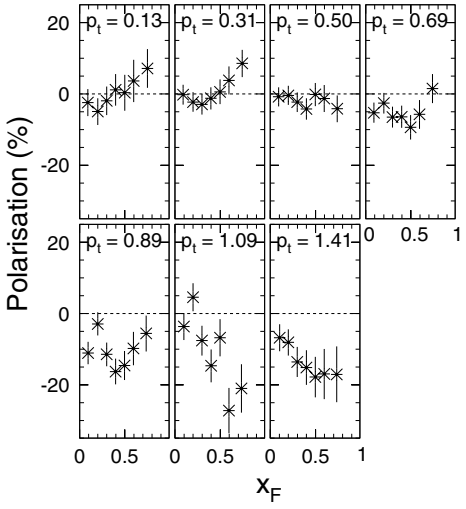


**Fig. 5.** Polarizations (in %) as a function of $x_F$ for fixed bins in $p_t$. The mean values of $p_t$ (in GeV/c) are indicated

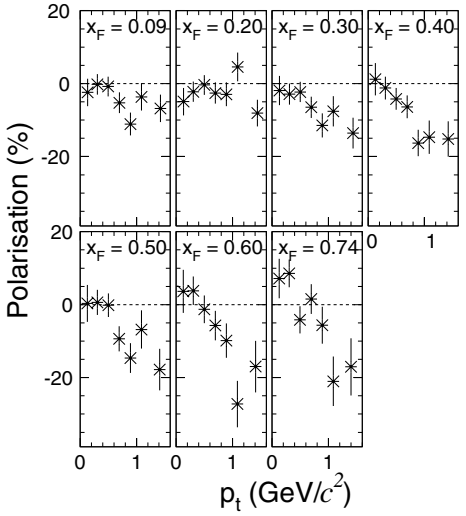


**Fig. 6.** Polarizations (in %) as a function of $p_t$ (in GeV/c) for fixed bins in $x_F$. The mean values of $x_F$ are indicated

number of $x_F/p_t$ bins from 49 to 16. Figure 7(left) shows the distribution of the differences $\Delta P = P(Cu) - P(C)$ normalized to their statistical errors. The mean value of the distribution is $-0.22 \pm 0.20$ and its r.m.s. is 0.78, in agreement with the hypothesis of purely statistical fluctuations. Figure 7(right) shows the polarization differences as a function of $x_F$. No significant copper/carbon target difference is visible.

## 6 Discussion

The results presented here constitute a fully two-dimensional study of the $x_F$ and $p_t$ dependence of $\Xi^-$ polarization, extending considerably the $x_F/p_t$ range of earlier $\Xi^-$ polarization measurements in proton and neutral beams [9–11].

The negative sign of the $\Xi^-$ polarization comes as no surprise. It is expected in the fragmentation/recombination

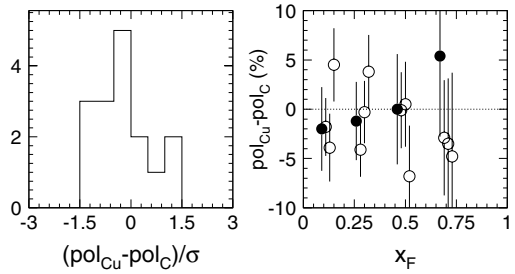


**Fig. 7.** Cu/C target comparison: The left-hand plot shows the distribution $\Delta\,\mathrm{pol}\,/\sigma$ for the 16 $x_F/p_t$ samples. There are no overflows. The right-hand plot shows $\Delta\,\mathrm{pol}$ (in %) vs $x_F$. For each value of $x_F$, four points are given corresponding to $p_t$ = 0.19 (solid) and 0.45, 0.73, 1.15 (open), respectively

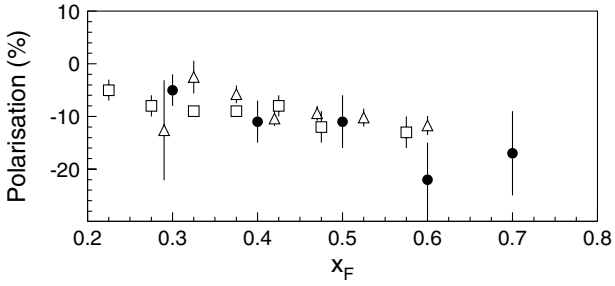


**Fig. 8.** Polarizations in units of % of $\Lambda$ (squares) and $\Xi^-$ (triangles) produced by protons and of $\Xi^-$ produced by $\Sigma^-$ (circles), at 5 mrad production angle, as a function of $x_F$

model of DeGrand and Miettinen [12], though there are no quantitative predictions available. In Fig. 8 we show the polarizations of $\Lambda$ and $\Xi^-$ produced inclusively by a proton beam of 400 GeV/c momentum in a beryllium target [8,9] at a production angle of 5 mrad and our data interpolated to the same production angle. The three data sets are very similar.

The polarization of $\Xi^-$ produced by $\Xi^-$ is unknown, therefore we cannot make any correction for the contribution from $\Xi^-$ interactions. However, in the region $0.4 < x_F < 0.6$, where the strong negative polarization at large $p_t$ is already fully developed, the fraction of $\Xi^-$ produced by $\Xi^-$ is between 0.1 and 0.2 only, therefore the polarization in this region is essentially due to $\Xi^-$ production by $\Sigma^-$. At the highest value $x_F = 0.75$, about 1/3 of the $\Xi^-$ are produced by $\Xi^-$, and the polarizations due to production by $\Sigma^-$ may differ significantly from our measured values.

The indication of a positive polarization at high $x_F$ and low $p_t$ is unexpected, but the effect is not very significant and clearly in need of verification.

A fraction of about 15% at low $x_F$ and 20% at high $x_F$ of the $\Xi^-$ sample was produced via the $\Xi^0(1530)$ and $\Xi^-(1530)$ resonances, as determined from the $\Xi^0(1530)$ production cross section measured in our experiment [20]. We cannot, however, extract a sufficiently clean sample of $\Xi^-$ produced in $\Xi^0(1530) \to \Xi^-\pi^+$ decays for a separate polarization analysis, and thus we can make no statement about the effects of $\Xi^-$ production via $\Xi^*$ resonances.

No dependence of the polarization on the target material was found.

*Acknowledgements.* It is a pleasure to thank J. Zimmer and G. Konorova for their support in setting up and running the experiment. We are also indebted to the staff of the CERN Omega spectrometer group for their help and support, to the CERN EBS group for their work on the hyperon beam line and to the CERN accelerator group for their continuous efforts to provide good and stable beam conditions. We also thank B. Friedgen of TU München for his help with preparing our final data tapes. Yu.A. Alexandrov gratefully acknowledges support by the Deutsche Forschungsgemeinschaft and the Russian Foundation for Basic Research under the contract number 436 RUS 113/465.

## References

1. J. Félix, Mod. Phys. Lett. A **12**, 363 (1997)
2. A. Bravar, Proc. Conf. High energy spin physics, Protvino 1998, 167
3. J. Félix, Mod. Phys. Lett. A **14**, 827 (1999)
4. J. Soffer, hep-ph/9911373 and Proc. Hyperon 99, Batavia, Illinois, Sept. 1999, p. 121
5. V.V. Abramov, hep-ph/0111128 (2001)
6. M.I. Adamovich et al., Eur. Phys. J. **C 32**, 221 (2004)
7. M.I. Adamovich et al., Z. Physik A **350**, 379 (1995)
8. K. Heller et al., Phys. Rev. Lett. **51**, 2025 (1983)
9. R. Rameika et al., Phys. Rev. D **33**, 3172 (1986)
10. J. Duryea et al., Phys. Rev. Lett. **67**, 1193 (1991)
11. D.M. Woods, Phys. Rev. D **54**, 6610 (1996)
12. T.A. DeGrand and H.I. Miettinen, Phys. Rev. D **23**, 1227 (1981), D **24**, 2419 (1981)
13. Yu.A. Alexandrov et al., Nucl. Instr. Methods A **408**, 359 (1998)
14. W. Beusch, CERN/SPSC/77-70
15. The Particle Data Group: K. Hagiwara et al., Phys. Rev. D **66**, 010001-65 (2002)
16. M.I. Adamovich et al., Z. Physik C **76**, 35 (1997)
17. S. Barlag et al., Phys. Lett. B **325**, 531 (1994)
18. R.T. Edwards et al., Phys. Rev. D **18**, 76 (1978)
19. S.F. Biagi et al., Z. Physik C **34**, 187 (1987)
20. M.I. Adamovich et al., Eur. Phys. J. C **11**, 271 (1999)